

ON THE INFLUENCE OF THE INITIAL ΔK LEVEL ON THE POST OVERLOAD CRACK PROPAGATION BEHAVIOUR

N. Ranganathan, J. Petit and J. de Fouquet

Ecole Nationale Supérieure de Mécanique et d'Aérotechnique, E.R.A. C.N.R.S. 123, 86034, Poitiers, France

ABSTRACT

The influence of the initial ΔK level on the fatigue crack retardation process has been studied in a large range of ΔK , on a 2024 aluminum alloy. Experimental results show that in the low ΔK regime where plane strain conditions predominate, microstructural factors govern the high delay observed. In the mid ΔK range a transition from plane strain to plane stress conditions leads to a minimum delay. At high ΔK values the progressive development of a plane stress regime at the crack tip induces a delay increase.

KEYWORDS

Fatigue crack propagation, overload, plane strain, plane stress, plastic zone, delay, grain size, threshold.

INTRODUCTION

It is now a well documented fact that the application of an overload can cause a significant decrease in the fatigue crack propagation rate and in some cases can even lead to complete crack arrest (Corbly, 1973 ; Wei, 1980 ; Probst, 1973). Models proposed earlier have helped in bringing out the mechanistic factors governing the retardation effect. But a unified approach is yet to emerge (Wheeler, 1970 ; Willenborg, 1971 ; Matsuoka, 1976 ; Elber, 1970) and the models cannot thoroughly explain the evolutions of the crack growth rate in the overload affected zone (Suresh, 1983). It has been previously reported that the application of a tensile overload can lead to four types of crack growth behaviour (Bernard, 1977). These are termed as :

- i - No effect
- ii - Immediate retardation
- iii - Delayed retardation following a slight acceleration
- iv - Lost retardation in which case the crack reaches a growth rate higher than the base line one before attaining the stable regime.

The retardation effects observed in a large range of ΔK on a high strength aluminum alloy in air and in vacuum are presented here to provide further phenomenological understanding of the post overload crack behaviour.

EXPERIMENTAL DETAILS

The material used was the 2024 Aluminum alloy in the T351 condition with two average grain sizes measured on the surface, Series I - 28 μm \times 45 μm , Series II - 60 μm \times 100 μm .

The nominal composition and mechanical properties, are listed in Table I. The 10 mm or 4 mm thick and 75 mm wide compact tension specimens were so oriented to have crack growth parallel to the longest grain dimension. The specimen surface was polished up to 1 μm to facilitate crack length measurement using a travelling microscope (resolution 0.01 mm).

Element	Si	Fe	Cu	Mn	Mg	Cr	Zn	Ti	Al
Percentage	0.10	0.22	4.46	0.66	1.50	0.01	0.04	0.02	Rest.

Table Ia - Nominal chemical composition

Orientation	Yield Strength MPa	Ultimate Strength MPa	Elongation %
LT	320	473	17.5
L	365	475	16.5

Table Ib - Average mechanical properties, specified by the supplier

The tests were conducted in load control conditions on a 5000 N electrohydraulic testing machine coupled with a PDP 11 computer. Test frequencies were typically 20 Hz in air and 35 Hz in vacuum (Petit, 1980). For all the tests the load ratio used was 0.1 and the overload ratio defined as the ratio of the peak load range to the initial cyclic load range was very near 2.

After the tests the specimen surfaces were examined under interferential contrast to analyse the development of the plastic zones and the behaviour of the crack in the overload affected region.

EXPERIMENTAL RESULTS AND ANALYSIS

A - Retardation behaviour :

In table 2 and 3 giving the test results the following parameters are defined starting from the left.

- No = Test Number
- ΔK_i = Stress intensity factor range before the overload.
- K_p = Stress intensity factor corresponding to the overload.
- a_d^p = Crack growth necessary to grow out of the overload affected region measured up to the point where the stable crack growth rate was again reached (Ranganathan, 1979).
- a^* = Crack growth after overload up to the point of minimum growth rate $(da/dN)_{\text{min}}$
- N_d = Number of delay cycles associated with a_d .
- DF = Delay factor $(da/dN)_i / (da/dN)_{\text{min}}$.

- Type = Type of delay curve, defined further down.

- Calculated plastic zone sizes in plane stress (CP) and plane stress (DP) in the following order :

- $2r^p$ = monotonic zones due to overload,
- $2r^y$ = monotonic zones before the overload,
- $2r^c$ = cyclic zones before the overload.

The formula used is : $2r = 1/\alpha\pi [K_{\text{max}}, K_p \text{ or } \Delta K_i / n \sigma_y]^2$

Where $\alpha = 1$ (CP) or 3 (DP)

σ_y = yield strength of the material

$n = 1$ (monotonic plastic zones) or 2 cyclic zones)

The plastic zones so calculated can be compared to the characteristic lengths a_d and a^* .

No	ΔK_i	K_p	a_d	a^*	$N_d \times 10^4$	DF	Type	$2r^p$		$2r^y$		$2r^c$	
								(CP)	(DP)	(CP)	(DP)	(CP)	(DP)
A1 ^o	5.6	11.8	-	-			A	0.44	0.15	0.12	0.04	0.02	0.008
A1 ^o	7.0	14.8	0.18	0.04	10.0	16	B	0.68	0.23	0.19	0.06	0.04	0.01
A2 ^o	8.0	16.9	0.7	0.05	4.5	42	B	0.89	0.30	0.25	0.08	0.05	0.02
A3 ^o	10.0	21.1	0.3	0.25	2.0	11	C	1.39	0.46	0.38	0.13	0.08	0.03
A4 ^o	12.6	26.6	0.9	0.30	1.5	14	C	2.19	0.73	0.61	0.20	0.12	0.14
A5 ^o	15.7	33.1	1.7	0.70	2.5	80	D	3.40	1.13	0.94	0.31	0.19	0.06
A6 ^o	18.9	39.9	4.7	0.83	4.0	111	D	4.94	1.65	1.37	0.46	0.28	0.09
A7 ^o	12.7	26.8	1.2	0.26	1.7	11	C	2.23	0.75	0.62	0.21	0.13	0.04
A8*	13.5	28.5	1.13	0.50	1.6	64	D	2.52	0.84	0.70	0.23	0.14	0.05
A9*	15.7	33.1	3.11	0.60	4.2	57	D	3.41	1.14	0.95	0.32	0.19	0.06
A10*	20.2	42.0	4.4	2.20	5.5	57	D	5.65	1.89	1.57	0.52	0.32	0.11
A11													

Table 2 - Experimental Results - Air (^o-Series I ; * - Series II)

No	ΔK_i	K_p	a_d	a^*	$N_d \times 10$	DF	Type	$2r^p$		$2r^y$		$2r^c$	
								(CP)	(DP)	(CP)	(DP)	(CP)	(DP)
V1 ^o	15.7	33.1	1.6	0.45	2.7	98	D	3.4	1.13	0.94	0.31	0.19	0.06
V2 ^o	18.9	39.9	4.9	0.55	1.7	257	E	4.9	1.6	1.4	0.46	0.28	0.09
V3*	12.7	26.8	1.0	0.32	0.93	162	C	2.23	0.74	0.6	0.21	0.13	0.04
V4*	13.5	28.5	2.0	0.41	1.7	383	D	2.52	0.84	0.7	0.23	0.14	0.05
V5*	15.7	33.1	3.4	0.56	2.7	174	D	3.5	1.13	0.94	0.31	0.19	0.06
V6*	18.5	39.0	2.8	1.65	4.1	356	D	4.7	1.58	1.32	0.44	0.27	0.09
V7*	21.0	44.3	7.2	3.70	4.2	487	D	6.1	2.03	1.69	0.56	0.34	0.11

Table 3 - Experimental Results - Vacuum (^o - Series I , * - Series II)

Units : $\Delta K_i, K_p$. MPa $\sqrt{\text{m}}$; $a_d, a^*, 2r_{p,y,c}$ mm

B - Types of delay curve

As mentioned in tables 2 and 3, five types of delay behaviours have been obtained according to the ΔK_i level.

Type A - Crack arrest following the overload observed at the lowest value of ΔK_i , i.e. $5.6 \text{ MPa}\sqrt{\text{m}}$ (test A_1°). No further crack growth is detected after 1.3×10^6 cycles following the application of the overload.

Type B - (Fig.1) - Obtained in the range $7.0 < \Delta K_i < 8.0 \text{ MPa}\sqrt{\text{m}}$. The overload causes a very slight crack advance after which the crack remains blocked before reacclerating to reach its preoverload growth rate. The number of cycles during which the crack is blocked is 35000 cycles for the lower ΔK_i value and 16500 cycles for the higher one.

Type C - (Fig.2) - Observed in the range $10.0 < \Delta K_i < 13.5 \text{ MPa}\sqrt{\text{m}}$. The crack growth rate following the overload is at first accelerated, then decelerates gradually to reach $(da/dN)_i$. The reaccleration process after this point is sudden and the crack growth rate reaches its preoverload value immediately.

Type D - (Fig.3) - Observed in the range $13.5 < \Delta K_i < 20.2 \text{ MPa}\sqrt{\text{m}}$ in air and $13.5 < \Delta K_i < 21 \text{ MPa}\sqrt{\text{m}}$ in vacuum in 10 mm thick specimens. The overload is characterized by a transient acceleration followed by a gradual deceleration and then a gradual reaccleration of the crack growth. This kind of behaviour is known as delayed retardation (Corbly, 1973 ; Ranganathan, 1979).

Type E - (Fig.4) - This type has been observed in vacuum and on a 4 mm thick specimen (test V_2°). In this case while the initial part of the reatardation curve is similar to type D, the final acceleration phase is characterized by a dip in the crack growth rate before the stable regime is reached.

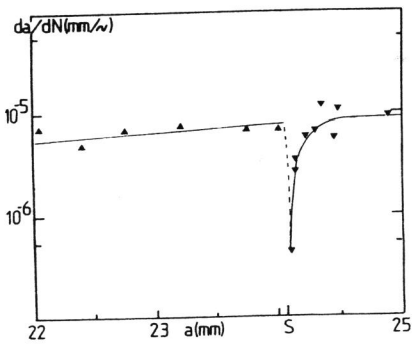


Fig.1 - Type B - Retardation curve test A_2° , S - overload application point.

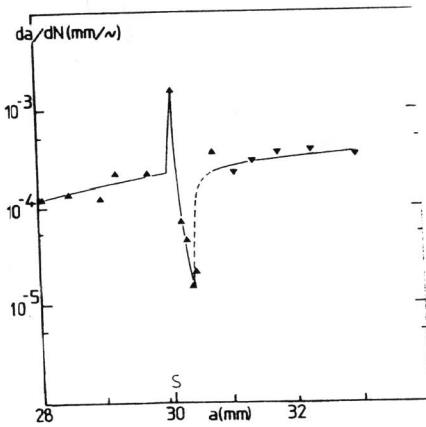


Fig.2 - Type C - Retardation curve test A_4°

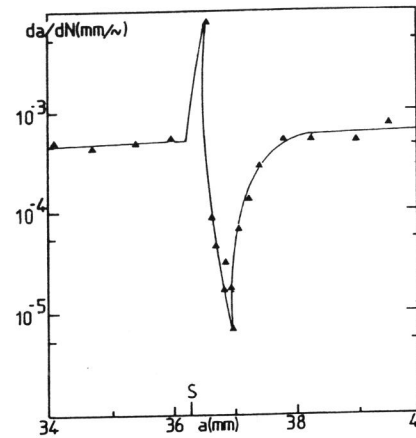


Fig.3 - Type D - Retardation curve test A_6° .

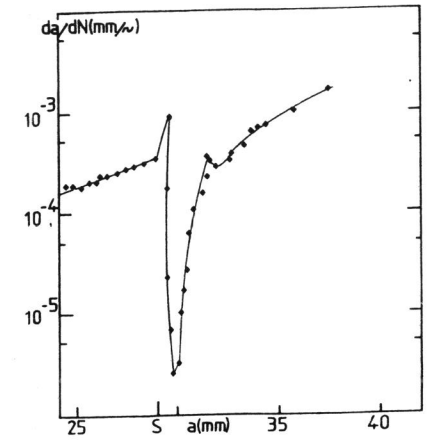


Fig.4 - Type E - Retardation curve test V_2° .

C - Crack behaviour in the overload affected zone

Fig.5 shows the development of the plastic zone for the tests V_5^* where a type D delay curve is obtained. The points corresponding to the beginning of the different stages in the delay process are indicated. As seen, the overload plastic zone is characterized by two wings, and in the deceleration phase the crack tip plastic zone diminishes to reach a minimum size for a crack growth approximately equal to a^* before increasing as the crack grows out of the overload affected zone.

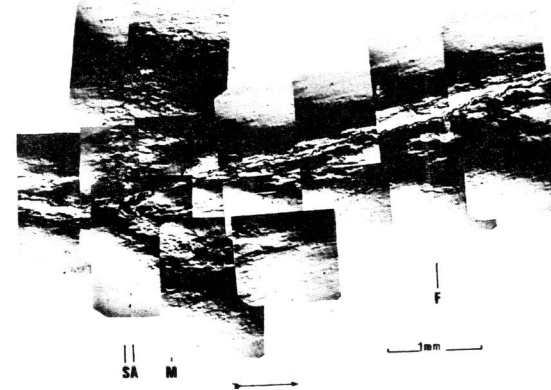


Fig.5- Plastic zone development. Test V_5^*
S - overload application point,
A - end of initial acceleration
M - Point of minimum growth rate,
F - end of affected region.

In the case of the test V_2° where a type E curve was observed, it has been seen that while the evolution of the plastic zone in the initial stages is similar to the previous case, at the beginning of the final stage the current plastic zone interacted with one wing of the overload plastic zone.

DISCUSSION

Evolution of the delay parameters and its significance

In the low ΔK_i range $< 10.0 \text{ MPa}\sqrt{\text{m}}$ the crack growth rate is strongly dependent on the microstructure and it can vary from one grain to another depending on its orientation (Petit, 1982, Kirby, 1979). The error in the determined a_d value is on the order of grain size, the average value indicated in table 2 is approximately equal to the plane strain overload plastic zone associated with K_p . At higher ΔK_i values, the values of a_d is in the range $2r_{pp} < a_d < 2r_{cp}$, and tends towards $2r_{cp}$ at the highest levels of ΔK_i considered here. The Fig. 6 shows the variation of N_d with ΔK_i for tests A_1 to A_7 . It can be seen that N_d which is very high for low ΔK_i values reaches a minimum of 15000 cycles for a ΔK_i of $12.6 \text{ MPa}\sqrt{\text{m}}$ before increasing for higher ΔK_i values. Such a "U" shaped curve has been attributed to a predominance of plane strain mode on the left hand side to a predominance of plane stress conditions on the right hand side (Veechio 1983).

Using the criterion given in (Knott 1973) the transition for plane strain to plane stress can be assumed to occur for a value of $K_{t,trans} = \sigma \sqrt{t/2.5}$ which gives for the 10 mm thick specimen a value of $20.24 \text{ MPa}\sqrt{\text{m}}$. For the test conditions studied, that is for $R = 0.1$ and for an overload ratio, $\tau = 2.0$ we have $K_p/\Delta k_i = 2.11$. Considering that the transition occurs when K_p attains $K_{t,trans}$, it corresponds to $\Delta K_i = 10.65 \text{ MPa}\sqrt{\text{m}}$. This result corroborates the above discussion on the a_d values.

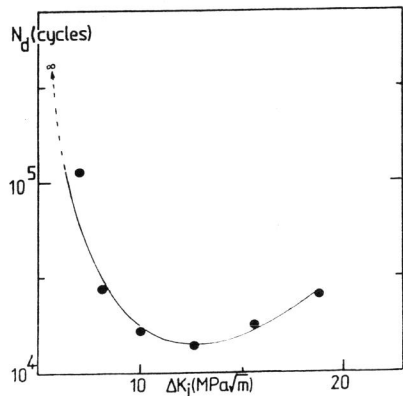


Fig.6 - Evolution of Number delay cycles with ΔK_i .

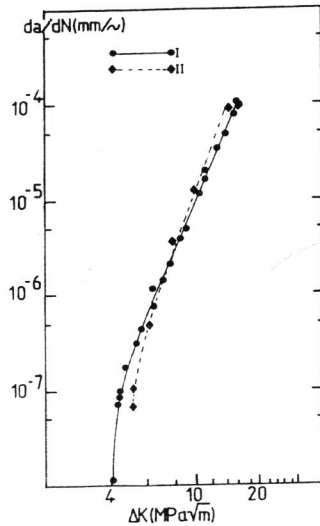


Fig.7 - Near threshold behaviour for series I and II in vacuum.

Concerning the a^* values, it can be seen from the table 2 that in the range $\Delta K_i < 8.0 \text{ MPa}\sqrt{\text{m}}$, a^* is comparable to the cyclic zone in plane stress. In the range $10.0 < \Delta K_i < 12.6 \text{ MPa}\sqrt{\text{m}}$, there is a sudden increase in a^* which reaches the order of a grain size. In the range $13.50 < \Delta K_i < 18.9 \text{ MPa}\sqrt{\text{m}}$, a^* values are intermediate between $2r_{cp}$ and $2r_{pp}$, a^* being greater than $2r_{pp}$ for the highest value of ΔK_i considered, $20.20 \text{ MPa}\sqrt{\text{m}}$. These observations are in accordance with the one reported in (Wei, 1980).

It can be noticed that the series II specimens have generally a more pronounced delay for comparable values of ΔK_i , corresponding to a higher grain size. It has been previously reported that near threshold conditions exist at the crack tip following the overload (Ranganathan 1979, Lankford 1982). Two series of tests were run to study the near-threshold conditions on the two grain sizes. As seen in Fig.7 the $\Delta K_{i,th}$ is lower for series I in vacuum, a similar behaviour being observed in air. Such a dependence of $\Delta K_{i,th}$ on grain size has been reported (Beevers, 1977). Now considering that for the same overload the change in the crack tip intensity factors is on the same order for the two series of specimens, the higher delay factor observed in serie II can be attributed to the conditions being closer to the threshold stress intensity range (Lankford, 1977).

Types of delay behaviour

It has been shown that at least five types of delay behaviour can be observed after overload, the type A, B and C corresponding to the left hand side of the U shaped curve in fig.6. For types A and B calculated plane strain plastic zone sizes $2r_{pp}$ and $2r_{cp}$ are typically smaller than the grain size. It should be noticed that the model proposed in (Mc Klintock, 1965) assumes a circular zone in plane strain while as reported in (Lankford 1977) the plastic zone size in the crack propagation direction can be in fact 4-5 times smaller than in the maximum size direction. In the case of type A behaviour it can be assumed that the effective crack tip stress intensity following the overload leads to a ΔK value at the crack tip smaller than the threshold inducing the crack arrest.

At higher ΔK_i values corresponding to type B curves where the crack remains blocked for a considerable time, and then suddenly progresses, the number of cycles during which the crack is blocked can be associated to the time necessary to induce new fatigue damage at the crack tip. Once this process is over the stable regime is reached after a crack growth of the order of 1 grain as indicated by the a_d values.

Type C behaviour is characterized by a substantial increase in a^* value (from $\approx 0.05 \text{ mm}$ in type B to $\approx 0.3 \text{ mm}$ in type C). The minimum delay observed in this case corresponds to the fact that the crack is not blocked at all after the deceleration period, the reacceleration taking place over a length of the order of 1 grain. After the transition point in fig. 6 is passed, typically type D curves are observed. This behaviour is characteristic of development of plane stress conditions with a large overload plastic zone affecting several grains and corresponding to deformation levels of the order of 5% plastic strain at the crack tip (Ranganathan, 1981). In this case it has been shown that the observed delay can be explained by a residual stress effect (Matsuoka 1976, Ranganathan 1981).

In type E curve it has been seen that the dip in the final acceleration phase is due to the interaction of the crack with one wing of the plastic zone. Indeed, in vacuum the wings of the plastic zone are seldom symmetrical with respect to the crack plane and crack deviation after overload is more often observed than in air (Verkin 1979).

CONCLUSIONS

This study has shown that five types of delay behaviour can be observed according to the initial ΔK level for the same overload ration. The conditions for their occurrence and the governing factors are :

Low ΔK region : high delay and even crack arrest, under plane strain condition, the microstructural factors playing an important role.

Mid ΔK region : minimum delay corresponding to a predeformed fatigue zone of the order of 1 grain and to the transition from plane strain to plane stress conditions at the crack tip.

High ΔK region : more pronounced delay associated with the plane stress conditions developed at the crack tip, and residual stress effect.

REFERENCES

- 1 - Beevers, C.J. Metal Science, 11, 1977, p. 362.
- 2 - Bernard, P.J. et al, Metal Science, 1977, p. 390.
- 3 - Corbly, D.M. and Packman, P.F., Engng. Fract. Mech. 6, 1973, p. 473.
- 4 - Elber, W., Engng. Fract. Mech., 2, 1970, p. 37.
- 5 - Kirby, B.R. and Beevers, C.J., Fatigue of Engng. Mat. and struct., 1, 1979, p. 203.
- 6 - Knott, J.F., Fundamentals of Fracture Mech. Eds. Butterworths, London, 1973.
- 7 - Lankford, J. and Davidson, D.L., Proceedings of 5th ICF Conference, Cannes, 2, 1982, p. 899.
- 8 - Lankford, J et al, ASTM STP 637, 1977, p. 36.
- 9 - Matsuoka, S. et al., Engng. Fract. Mech. 8, 1976, p. 507.
- 10 - Mc Clintock, F.A. and Irwin, G.R., ASTM STP 381, 1965, p. 84.
- 11 - Petit, J. et al, Revue de Phys. Appliquée, 15, 1980, 919.
- 12 - Petit, J. et al, Proceedings of the 4th ECF Conference, Leoben, Eds. EMAS, Warley U.K., 2, 1982, p. 426.
- 13 - Probst, E.P. and Hillberry, B.M., AIAA Journal, 73, 1973, p. 325.
- 14 - Ranganathan, N. et al., Engng Fract. Mech. 11, 1979, p. 775.
- 15 - Ranganathan, N. and Petit, J., ASTM STP 811
- 16 - Ranganathan, N. et al, Proceedings of 2nd ECF Conference, Darmstadt, VDI-Z, 18, 1979, p. 337.
- 17 - Ranganathan, N et al, Proceedings, 8th Congress on Material testing Budapest, 1, p. 309, 1981.
- 18 - Suresh, S., Engng. Fract. Mech., 18, 1983, p. 577.
- 19 - Verkin, B.I. and Grinberg, N.M., Mat. Sci. Engng., 41, 1979, p. 149.
- 20 - Vecchio, R.S. et al, Scripta Met., 17, 1983, p. 343.
- 21 - Wei, R.P., et al., J. Engng. Mat. Tech., Trans. ASME, 102, 1980, p. 280.
- 22 - Wheeler, O.E., General Dynamics Report, FZM-5602, 1970.
- 23 - Willenborg, J. et al, Tech. Rep. TFR 71-701, Log Angeles Division, North American Rockwell, 1971.